Coupling Coefficient Between Microstrip Line and Dielectric Resonator

YASUTOSHI KOMATSU AND YOSHIKAZU MURAKAMI

Abstract—**A formula of the coupling coefficient between a dielectric resonator and a microstrip line is derived from an analysis of the transmission characteristics of the microstrip line coupled to the dielectric resonator. A practical method of calculation is developed using Fourier analysis. The calculated values show good agreement with the experimental values.**

I. Introduction

Dielectric resonators, offering high-Q cavity performance in microwave integrated circuits, are widely used in filters, stabilized oscillators, discriminators, and so on [1]–[3]. When a dielectric resonator is placed beside a microstrip line and magnetically excited, this structure works as a band-stop filter just like a structure consisting of a waveguide and a series-connected reaction-type cavity. These two structures, therefore, have been considered to be represented by the identical equivalent circuits, i.e., the parallel resonance circuits [2]–[6]. The coupling coefficient between the dielectric resonator and the microstrip line is indispensable to determine the equivalent circuit parameters. This coupling coefficient has been formulated in some papers [7], [13]. Those formulations, however, do not explain the propriety of the above equivalent circuit, since they integrated the coupling energy between an electromagnetic field due to the resonator and the field due to the microstrip line within a volume of the resonator.

In this paper, a simple formula of the coupling coefficient is derived from an analysis of the transmission characteristics of a microstrip line coupled to a dielectric resonator. Because of this approach, the parallel resonance equivalent circuit naturally results, and the derived formula has the further advantages of including only the line integral instead of the volume integral and clearly expressing the effect of the line, which was not explicitly expressed in the previously mentioned formulas.

A practical method of calculating the coupling coefficient by means of Fourier analysis and experimental results are also presented. The agreement between theory and experiment is shown to be very good.

II. Analysis

When a dielectric resonator is placed in the vicinity of a microstrip line, as shown in Fig. 1, and excited in the $TE_{01\delta}$ mode, the transmission characteristics are modified by the

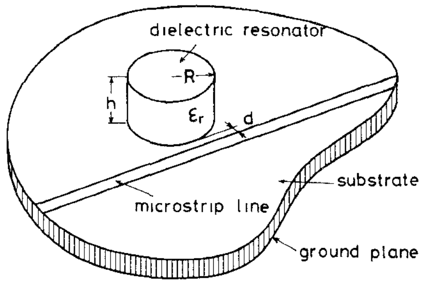

Fig. 1. A dielectric resonator coupled with a microstrip line.

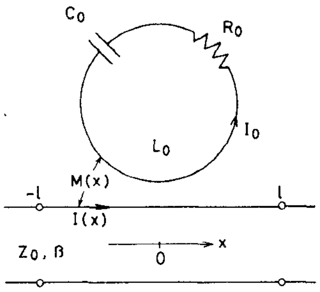

Fig. 2. A conducting loop coupled with a transmission line.

magnetic effect. The electric effect caused by the high dielectric constant of the dielectric resonator can be assumed to be very small since most of the electric field of the microstrip line is not only concentrated under the microstrip but also almost orthogonal to the electric field of the resonator [4]. The magnetic effect is an interaction between the magnetic field of the resonator and the magnetic field owing to the current in the microstrip line. This interaction can be regarded as mutual inductance, and an electromotive force is considered to be caused in the microstrip line. Thus the transmission characteristics of the microstrip line forced by this electromotive force should be analyzed first.

The analysis is made on the following assumptions.

1) The width of the microstrip is much smaller than the diameter of the dielectric resonator.

2) The microstrip line carries only the TEM mode.

3) The dielectric resonator can be represented by a conducting loop having in series an inductance L_0, a capacitance C_0, and a resistance R_0. The resonance occurs at the angular frequency $\omega_0 = 1/\sqrt{L_0 C_0}$ [8].

4) Only the $TE_{01\delta}$ mode is strongly excited and field distortion caused by other modes is very small [4], [13].

5) The dielectric resonator couples with the microstrip

Manuscript received November 11, 1981; revised August 30, 1982.
The authors are with the Sony Corporation Research Center, Yokohama, 240, Japan.

line through the distributed mutual inductance.

With these assumptions, the structure of Fig. 1 can be represented by a resonance circuit magnetically coupled with a transmission line, as shown in Fig. 2, where $M(x)$ indicates the distributed mutual inductance per unit length along the X-axis. From the assumption 4), if the effect of only the $TE_{01\delta}$ mode is considered, the electromagnetic field pattern is considered symmetric with respect to the axis which is perpendicular to the microstrip line and passes through the center of the dielectric resonator. It is convenient to set the origin of the X-axis on this axis of symmetry so that $M(x)$ can be regarded as an even function.

First, let us suppose that $M(x)$ is null outside the interval $-l$ to $+l$ in order to make the following argument clear, though $M(x)$ is usually considered to decrease gradually along the microstrip line. Let $I(x)$ and I_0 be the current on the transmission line and the resonance circuit, respectively. Since the electromotive force induced on the transmission line can be expressed as $-j\omega M(x)I_0$, a modified differential equation of a transmission line is obtained as follows:

$$\frac{d^2I(x)}{dx^2} = -\omega^2 LC\left(I(x)+\frac{M(x)I_0}{L}\right) \tag{1}$$

where L and C are the inductance and capacitance per unit length of the transmission line, respectively. Since $M(x)$ is assumed to be null outside the interval $-l$ to $+l$, the following equation is given by the reciprocal condition:

$$j\omega\int_{-l}^{+l} M(x)I(x)\,dx + \left(j\omega L_0 + \frac{1}{j\omega C_0} + R_0\right)I_0 = 0. \tag{2}$$

Substituting (2) into (1) and using $\beta^2 = \omega^2 LC$, we obtain

$$\frac{d^2I(x)}{dx^2} = -\beta^2(I(x) - KM(x)) \tag{3}$$

where

$$K = j\frac{G}{LL_0}\cdot\frac{\omega}{\omega_0}\int_{-l}^{+l} M(x)I(x)\,dx \tag{4}$$

$$G = \frac{Q_0}{1 + jQ_0(\omega/\omega_0 - \omega_0/\omega)}. \tag{5}$$

Equation (3) is a well-known linear differential equation with a forcing function and the general solution is expressed as follows [9]:

$$I(x) = A\exp(-j\beta x) + B\exp(j\beta x) + \frac{j\beta K}{2}\left[\int_{-l}^{x} M(x)\exp(j\beta x)\,dx\right]\exp(-j\beta x) - \frac{j\beta K}{2}\cdot\left[\int_{-l}^{x} M(x)\exp(-j\beta x)\,dx\right]\exp(j\beta x). \tag{6}$$

Substituting (6) into (4), K is obtained as

$$K = \frac{j\left\{A\int_{-l}^{+l} M(x)\exp(-j\beta x)\,dx + B\int_{-l}^{+l} M(x)\exp(j\beta x)\,dx\right\}}{\frac{LL_0\omega_0}{G\omega} + \frac{\beta}{2}\int_{-l}^{+l}\left[\left\{\int_{-l}^{x} M(x)\exp(j\beta x)\,dx\right\}M(x)\exp(-j\beta x) - \left\{\int_{-l}^{x} M(x)\exp(-j\beta x)\,dx\right\}M(x)\exp(j\beta x)\right]dx}. \tag{7}$$

Considering that $M(x)$ is an even function, this can be simplified to

$$K = \frac{2j\eta(A+B)}{\gamma + j\beta\delta} \tag{8}$$

where

$$\gamma = (LL_0/G)\cdot(\omega_0/\omega), \qquad \eta = \int_0^l M(x)\cos(\beta x)\,dx$$

$$\delta = \int_{-l}^{+l}\left\{\int_{-l}^{x} M(x)\sin(\beta x)\,dx\right\}M(x)\cos(\beta x)\,dx - \int_{-l}^{+l}\left\{\int_{-l}^{x} M(x)\cos(\beta x)\,dx\right\}M(x)\sin(\beta x)\,dx.$$

Then the general solution (6) becomes

$$I(x) = \left[A - \frac{\beta\eta(A+B)}{\gamma + j\beta\delta}\int_{-l}^{x} M(x)\exp(j\beta x)\,dx\right]\cdot\exp(-j\beta x) + \left[B + \frac{\beta\eta(A+B)}{\gamma + j\beta\delta}\int_{-l}^{x} M(x)\cdot\exp(-j\beta x)\,dx\right]\exp(j\beta x). \tag{9}$$

Let us determine the S-parameters of the two-port network of Fig. 2 defined by $-l$ and $+l$ reference planes. First, the transmission line is supposed to be terminated by the characteristic impedance at $x = l$ to calculate S_{11} and S_{21}. This leads to the condition that the second term of (9) vanishes at $x = l$

$$B + \frac{\beta\eta(A+B)}{\gamma + j\beta\delta}\int_{-l}^{+l} M(x)\exp(-j\beta x)\,dx = 0. \tag{10}$$

The ratio of B to A can be obtained by solving (10)

$$\frac{B}{A} = \frac{\dfrac{-2\beta\eta^2}{\gamma + j\beta\delta}}{1 + \dfrac{2\beta\eta^2}{\gamma + j\beta\delta}}. \tag{11}$$

S_{11} and S_{21} can now be calculated by substituting (11) into (9)

$$S_{11} = -\frac{B}{A}\exp(-2j\beta l) = \frac{\dfrac{2\beta\eta^2}{\gamma + j\beta\delta}}{1 + \dfrac{2\beta\eta^2}{\gamma + j\beta\delta}}\exp(-j2\beta l) \tag{12}$$

$$S_{21} = \frac{A - \dfrac{\beta\eta(A+B)}{\gamma + j\beta\delta}\int_{-l}^{+l} M(x)\exp(j\beta x)\,dx}{A}\cdot\exp(-j2\beta l) = \frac{1}{1 + \dfrac{2\beta\eta^2}{\gamma + j\beta\delta}}\exp(-j2\beta l). \tag{13}$$

S_{22} and S_{12} can be obtained by taking the symmetry into account

$$\begin{cases} S_{11} = S_{22} \\ S_{21} = S_{12}. \end{cases} \tag{14}$$

These results show that if we are interested in the S-parameters of the two-port junction defined by the $-l$ and $+l$ reference planes, by bringing the reference planes to $x = 0$, the effect of the dielectric resonator can be represented by the two-port network at the origin whose scattering matrix is expressed as

$$[s]_0 = \begin{pmatrix} \dfrac{\dfrac{2\beta\eta^2}{\gamma + j\beta\delta}}{1 + \dfrac{2\beta\eta^2}{\gamma + j\beta\delta}} & \dfrac{1}{1 + \dfrac{2\beta\eta^2}{\gamma + j\beta\delta}} \\ \dfrac{1}{1 + \dfrac{2\beta\eta^2}{\gamma + j\beta\delta}} & \dfrac{\dfrac{2\beta\eta^2}{\gamma + j\beta\delta}}{1 + \dfrac{2\beta\eta^2}{\gamma + j\beta\delta}} \end{pmatrix}. \tag{15}$$

The two-port network having this scattering matrix is a series impedance Z located at $x = 0$ with the value of

$$Z = \frac{4\beta\eta^2}{\gamma + j\beta\delta}. \tag{16}$$

In the vicinity of the resonance frequency ω_0, this can be written as follows:

$$Z = \frac{4k_\eta^2 Q_0}{1 - \dfrac{\Delta\omega}{\omega_0} + j2Q_0\left(\dfrac{k_\eta^2\delta}{2\eta^2} + \dfrac{\Delta\omega}{\omega_0}\right)} \tag{17}$$

where $k_\eta = \eta/\sqrt{LL_0/\beta}$ and $\Delta\omega = \omega - \omega_0$. We introduce new parameters ω_0' and Q_0' here instead of ω_0 and Q_0 to further simplify (17)

$$\omega_0' = \omega_0\left(1 - \frac{k_\eta^2\delta}{2\eta^2}\right) \tag{18}$$

$$Q_0' = Q_0 \Big/ \left(1 + \frac{k_\eta^2\delta}{2\eta^2}\right). \tag{19}$$

Substituting (18) and (19) into (17), we obtain

$$Z = \frac{4k_\eta^2 Q_0'}{1 - \dfrac{\Delta\omega'}{\omega'}\dfrac{1}{1 + \dfrac{k_\eta^2\delta}{2\eta^2}} + j2Q_0'\dfrac{\Delta\omega'}{\omega_0'}} \tag{20}$$

where $\Delta\omega_0' = \omega - \omega_0'$. The term $(\Delta\omega'/\omega_0')/(1 + k_\eta^2\delta/2\eta^2)$ can be considered very small in the vicinity of ω_0. If we neglect this term, the following approximation will be obtained:

$$Z = \frac{4k_\eta^2 Q_0'}{1 + j2Q_0'\dfrac{\Delta\omega'}{\omega_0'}}. \tag{21}$$

An equivalent circuit having this impedance in series is

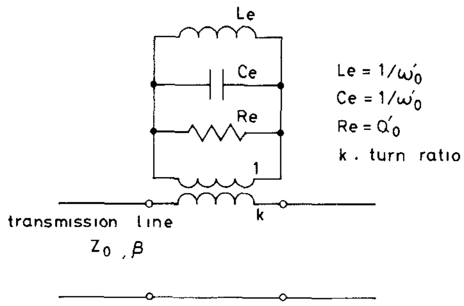

Fig. 3. A parallel resonant equivalent circuit of a dielectric resonator.

represented by a parallel resonance circuit, as shown in Fig. 3. The square of the turn ratio of the transformer, denoted by k^2, expresses the coupling strength between the dielectric resonator and the microstrip line. The expression of the k^2 can be obtained by comparing the impedance value of the equivalent circuit of Fig. 3 with (21)

$$k^2 = 4k_\eta^2 Z_0 = 4\omega\left[\int_0^{+l}\left(M(x)/\sqrt{L_0}\right)\cos(\beta x)\,dx\right]^2. \tag{22}$$

So far, we assumed that $M(x)$ is null outside the interval $-l$ to $+l$. However, if $M(x)$ can be considered to decay gradually along the microstrip line, we must then set the limit of the interval far away enough from the dielectric resonator to take all of $M(x)$ into account. In this case, the upper limit of the integral of k^2 can be replaced by ∞:

$$k^2 = 4\omega\left[\int_0^{\infty}\left(M(x)/\sqrt{L_0}\right)\cos(\beta x)\,dx\right]^2. \tag{22$'$}$$

The undetermined variables $M(x)$ and L_0 in (22) and (22)$'$ can be rewritten with other variables for practical calculation as follows. The electromotive force is induced on the microstrip line by the alternating magnetic field of the dielectric resonator. This magnetic field, however, is always accompanied by an electric field. The projection of this electric field in the X-direction, indicated by E_x, proves to be equal to the electromotive force from Maxwell's equations. Then we have

$$E_x = -j\omega M(x) I_0. \tag{23}$$

The average magnetic energy stored in the resonance field is considered to be equal to the average magnetic energy stored in the inductance in Fig. 2. This energy is given by

$$W = L_0 I_0^2/2. \tag{24}$$

Substituting (23) and (24) into (22)$'$, we consequently obtain

$$k^2 = \frac{2\omega}{W}\left(\int_0^{\infty}(E_x/j\omega)\cos(\beta x)\,dx\right)^2. \tag{25}$$

We can determine W and E_x from the resonance field of the dielectric resonator and we can calculate the value of k^2 from (25). The coupling coefficient β_0 between the resonance circuit and the transmission line is given by [10]

$$\begin{aligned}\beta_0 &= Q_0/Q_{\text{ext}} = Q_0 k^2/2Z_0 = 2k_\eta^2 Q_0 \\ &= \frac{2\omega Q_0}{Z_0}\left(\int_0^{\infty}\left(M(x)/\sqrt{L_0}\right)\cos(\beta x)\,dx\right)^2. \end{aligned} \tag{26}$$

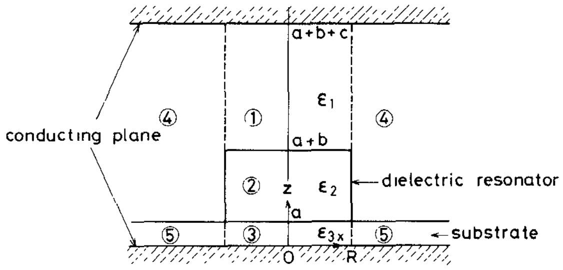

Fig. 4. Side view of a dielectric resonator on a substrate.

III. Method of Numerical Calculation

In this section, a method of calculating k^2 using (25) is developed. First, the expression of the resonance field has to be derived. For this, a structure consisting of a cylindrical dielectric resonator and a substrate, as shown in Fig. 4, is assumed. The microstrip line on the substrate is eliminated for simplification. The space between upper and lower conductors is divided into five regions. Since the electromagnetic field in the $TE_{01\delta}$ mode has only H_z, H_r, and E_θ components, it is represented in each region by a magnetic Hertz vector which is expressed by a product of a unit vector along the Z-axis and a scalar function [11]. This scalar function in each region can be expanded in the Fourier series as follows [12]:

$$\left\{\begin{aligned} \Phi_1 &= \sum_p A_{1p} J_0(k_p r) \sin\beta_{1p}(z-(c+b+a)) \\ \Phi_2 &= \sum_p A_{2p} J_0(k_p r) \sin\beta_{2p}(z+\delta_p) \\ \Phi_3 &= \sum_p A_{3p} J_0(k_p r) \sin\beta_{3p} z \\ \Phi_4 &= \sum_q B_q H_0(k_q r) \sin\beta_{4q}(z-(c+b+a)) \\ \Phi_5 &= \sum_q C_q H_0(k_q r) \sin\beta_{5q} z \end{aligned}\right. \tag{27}$$

where A_{1p}, A_{2p}, A_{3p}, B_q, C_q, and δ_p are constants to be determined and

$$\left\{\begin{aligned} k_p^2 &= (\omega/C_0)^2\epsilon_1 - \beta_{1p}^2 = (\omega/C_0)^2\epsilon_2 - \beta_{2p}^2 \\ &= (\omega/C_0)^2\epsilon_3 - \beta_{3p}^2 \\ k_q^2 &= (\omega/C_0)^2\epsilon_1 - \beta_{4q}^2 = (\omega/C_0)^2\epsilon_3 - \beta_{5q}^2. \end{aligned}\right. \tag{28}$$

J_0 and H_0 are the Bessel and the second Hankel functions of order zero. From the boundary condition that H_r and E_θ derived from (27) are continuous at $z = a$ and $a+b$, we obtain

$$\frac{\tan\beta_{1p}c}{\beta_{1p}} + \frac{\tan\beta_{2p}b}{\beta_{2p}} + \frac{\tan\beta_{3p}a}{\beta_{2p}} - \frac{\beta_{1p}}{\beta_{1p}\beta_{3p}}\tan\beta_{1p}c\cdot\tan\beta_{2p}b\cdot\tan\beta_{3p}a = 0 \tag{29}$$

$$\frac{\tan\beta_{4q}(c+b)}{\beta_{4q}} + \frac{\tan\beta_{5q}a}{\beta_{5q}} = 0. \tag{30}$$

Using β_{1p}, β_{2p}, β_{3p}, β_{4q}, and β_{5q} satisfying (29) and (30), we obtain the following relations:

$$\left\{\begin{aligned} &A_{3p}\sin\beta_{3p}a = A_{2p}\sin\beta_{2p}(a+\delta_p) \\ &A_{1p}\sin\beta_{1p}c = -A_{2p}\sin\beta_{2p}(b+a+\delta_p) \\ &\delta_p = \frac{1}{\beta_{2p}}\left[\tan^{-1}\left(\frac{\beta_{2p}}{\beta_{1p}}\tan\beta_{1p}c\right)\right] - b - a \\ &C_q\sin\beta_{5q}a = -B_q\sin\beta_{4q}(c+b). \end{aligned}\right. \tag{31}$$

Next, let us consider the following integrals to formulate the continuity condition on H_z and E_θ at $r = R$:

1)

$$\begin{aligned} &\int_0^a \Phi_5 C_q \sin\beta_{5q}z\,dz + \int_a^{c+b+a}\Phi_4 B_q\sin\beta_{4q}(z-c-b-a)\,dz \\ &= \left[\frac{C_q^2}{2}\left(a - \frac{\sin\beta_{5q}a\cdot\cos\beta_{5q}a}{\beta_{5q}}\right) + \frac{B_q^2}{2}\left((c+b) - \frac{\sin\beta_{4q}(c+b)\cdot\cos\beta_{4q}(c+b)}{\beta_{4q}}\right)\right]H_0(k_qR) \\ &= B_q^2 H_0(k_qR) I_q \end{aligned} \tag{32}$$

where

$$\begin{aligned} I_q = &\frac{-\beta_{4q}\sin\beta_{4q}(c+b)\cdot\cos\beta_{4q}(c+b)}{2\beta_{5q}\sin\beta_{5q}a\cdot\cos\beta_{5q}a} \cdot\left(a - \frac{\sin\beta_{5q}a\cdot\cos\beta_{5q}a}{\beta_{5q}}\right) \\ &+ \frac{1}{2}\left[(c+b) - \frac{\sin\beta_{4q}(c+b)\cdot\cos\beta_{4q}(c+b)}{\beta_{4q}}\right]. \end{aligned} \tag{33}$$

2)

$$\begin{aligned} &\int_0^a \Phi_3 C_q\sin\beta_{5q}z\,dz + \int_a^{b+a}\Phi_2 B_q\sin\beta_{4q}(z-c-b-a)\,dz \\ &+ \int_a^{c+b+a}\Phi_1 B_q \sin\beta_{4q}(z-c-b-a)\,dz \\ &= B_q\sum_p A_{2p}J_0(k_pR)J_{pq} \end{aligned} \tag{34}$$

where

$$\begin{aligned} J_{pq} = &\frac{\beta_{2p}^2 - \beta_{1p}^2}{(\beta_{2p}^2-\beta_{4q}^2)(\beta_{1p}^2-\beta_{4q}^2)} \\ &\times\left[\beta_{2p}\{\cos\beta_{2p}(a+\delta_p)\cdot\sin\beta_{4q}(c+b) - \cos\beta_{2p}(b+a+\delta_p)\cdot\sin\beta_{4q}c\}\right. \\ &\left. + \beta_{4q}\{\sin\beta_{2p}(a+\delta_p)\cdot\cos\beta_{4p}(c+b) - \sin\beta_{2p}(b+a+\delta_p)\cdot\cos\beta_{4q}c\}\right]. \end{aligned} \tag{35}$$

Equations (31) are used in these calculations. Applying the continuity condition of H_z and E_θ to (32) and (34), we obtain

$$\left\{\begin{aligned} &\sum_p A_{2p}k_p^2 J_0(k_pR)J_{pq} = B_q k_q^2 H_0(k_qR) I_q \\ &\sum_p A_{2p}k_p J_0'(k_pR)J_{pq} = B_q k_q H_0'(k_qR) I_q \end{aligned}\right. \tag{36}$$

where J_0' and H' indicate the derivatives of J_0 and H_0, respectively. Eliminating B_q from (36), we have

$$\sum_q X_p \left[k \frac{J_0(k_p R)}{p J_0'(k_p R)} - k \frac{H_0(k_q R)}{q H_0'(k_q R)} \right] J_{pq} = 0 \quad (37)$$

where

$$X_p = A_{2p} k_p J_0'(k_p R).$$

Equation (37) can be simplified as follows by introducing the new parameters H_{pq}:

$$\sum_p X_p H_{pq} = 0 \quad (38)$$

where

$$H_{pq} = \left[k \frac{J_0(k_p R)}{p J_0'(k_p R)} - k \frac{H_0(k_q R)}{q H_0'(k_q R)} \right] J_{pq}. \quad (39)$$

Equation (38) must be satisfied for each q. Since each Fourier series in (27) is an infinite series, (38) expresses a set of infinite number of homogeneous equations with an infinite number of unknowns. An approximation by truncating the series is possible, however, because the first few terms in each series are predominant. If first n terms are taken into account, a system of n homogeneous linear equations in n unknowns is obtained

$$\sum_{p=1}^{n} X_p H_{pq} = 0, \qquad q = 1, 2, \cdots, n. \quad (40)$$

When the rank of the system matrix $[H_{pq}]$ is equal to $n-1$, a solution of (40) is obtained as follows:

$$X_1 = \alpha[H]_{1k}, X_2 = \alpha[H]_{2k},$$
$$X_3 = \alpha[H]_{3k}, \cdots, X_n = \alpha[H]_{nk} \quad (41)$$

where α is an arbitrary constant and $[H]_{ij}$ is the cofactor of H_{ij} in the $\det[H_{pq}]$. Equation (40) is the formula of the boundary condition at $r = R$. If the solution (41) is obtained, all constants A_{1p}, A_{2p}, A_{3p}, B_q, C_q, and δ_p are determined from (31) and (36) with a constant α. All scalar functions in (27) can be calculated with these constants and β_{1p}, β_{2p}, β_{3p}, β_{4q}, and β_{5q} obtained from (28).

The time-average magnetic energy stored in the resonance field can now be calculated. The time-average electric energy which is equal to the magnetic energy, however, is much easier and more suitable for calculation than the magnetic energy in this case. The time-average electric energy is given by

$$W = \int_v \frac{\epsilon}{2} E_\theta E_\theta^* \, dv$$
$$= \frac{\omega^2 \mu^2}{2} \int_v \epsilon \left(\frac{\partial \Phi}{\partial r} \right) \left(\frac{\partial \Phi}{\partial r} \right)^* dv \quad (42)$$

where ϵ, μ, and Φ indicate the dielectric constant, permeability, and the scalar function in each region, respectively. Actually, W can be obtained by performing the integration over each region separately and summing them.

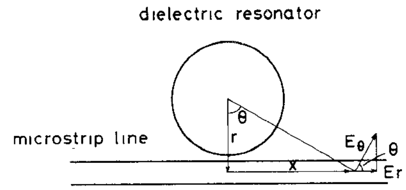

Fig. 5. Electric field along a microstrip line caused by the resonance field of a dielectric resonator.

E_x can also be expressed with E_θ, as shown in Fig. 5, by

$$E_x = E_\theta \cos\theta = E_\theta \left(r_0 / \sqrt{r_0^2 + x^2} \right)$$
$$= -j\omega\mu \left(r_0 / \sqrt{r_0^2 + x^2} \right) \left(\partial \Phi_4 / \partial r \right)_{y=-r, z=a}$$
$$= -j\omega\mu \left(r_0 / \sqrt{r_0^2 + x^2} \right) \frac{\partial}{\partial r}$$
$$\cdot \left[\sum_q B_q k_q H_0 \left(k_q \sqrt{r_0^2 + x^2} \right) \sin \beta_{4q}(c+b) \right]. \quad (43)$$

In the usual case, where $\epsilon_1 < \epsilon_3 < \epsilon_2$ and $a < b$, k_q's are all pure imaginary numbers and H_1 is replaced by K_1, the modified Hankel function of order 1. In this case, the integral in (25) is obtained from (43) as follows:

$$\int_0^\infty (E_x / j\omega) \cos\beta x \, dx = \mu \sum_q B_q' k_q' r \sin \beta_{4q}(c+b)$$
$$\cdot \int_0^\infty \frac{K_1 \left(k_q' \sqrt{r_0^2 + x^2} \right)}{\sqrt{r_0^2 + x^2}} \cos\beta x \, dx$$
$$= \frac{\pi\mu}{2} \sum_q B_q' \sin\beta_{4q}(c+b) \exp\left(-r_0 \sqrt{k_q'^2 + \beta^2} \right) \quad (44)$$

where $k_q' = -jk_q$ and

$$B_q' = \sum_p A_{2p} k_p J_1(k_p R) J_{pq} / k_q' K_1(k_q' R) I_q. \quad (45)$$

The right side of (45) consists of only determined variables, hence, we can calculate the right side of (44). Substituting (44) and (42) into (25), we can finally obtain the values of k^2. In this case, k^2 is a function of the size and ϵ of the resonator, ϵ of the substrate, and the distance between the line and the resonator.

IV. Comparison Between Theoretical and Experimental Values

The experiments were made with three kinds of cylindrical dielectric resonators made of zirconate ceramics. The 50-Ω microstrip line was fabricated on an alumina substrate 0.025 in thick, and a dielectric resonator was placed beside the line at a distance d (Fig. 1). The accuracy of d in the experiments was within 20 μm. Experimental values of k^2 were calculated from the transmission coefficients. The magnitude of the transmission coefficient S_{21} at $\omega = \omega_0$ is given from (21) as

$$|S_{21}|_{\omega=\omega_0'} = 1 / \left(1 + 2Q_0' k_\eta^2 \right). \quad (46)$$

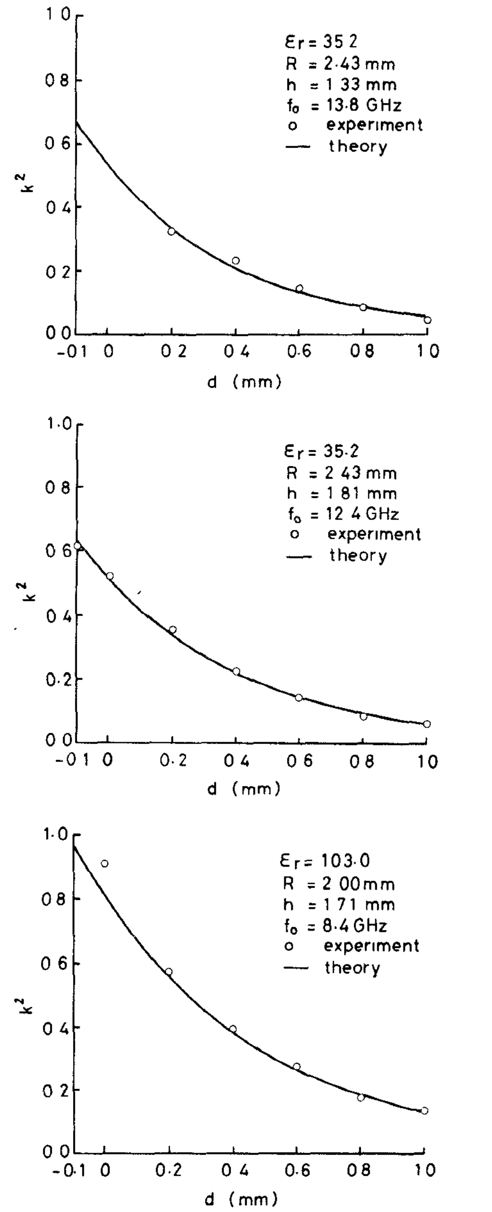

Fig. 6. The square of turn ratio k^2 versus the distance d between the edge of the dielectric resonator and the edge of the microstrip line for the various resonators, where the substrate thickness $a = 0.635$ mm and the air gap $c = 8.0$ mm.

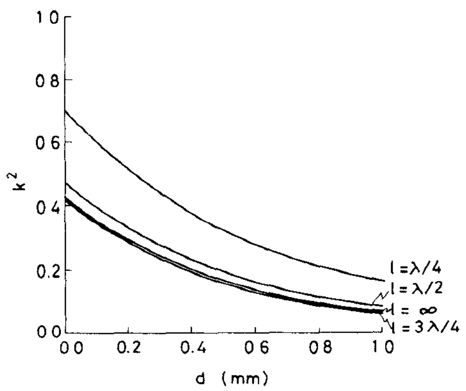

Fig. 7. Calculated k^2 values for limited length lines, where $a = 0.635$ mm, $b = 2.24$ mm, $c = 2.2$ mm, $R = 2.79$ mm, $\epsilon_1 = 1.0$, $\epsilon_2 = 29.8$, $\epsilon_3 = 10.0$, and $f_0 = 11.68$ GHz.

Then, from (22), we obtain

$$k^2 = 4k_\eta^2 Z_0 = \frac{2Z_0\left(1-|S_{21}|_{\omega=\omega_0'}\right)}{Q_0'|S_{21}|_{\omega=\omega_0'}}. \tag{47}$$

The transmission coefficient was measured around ω_0' by a network analyzer. The measured value, however, includes the effects of the transmission loss and of the impedance mismatch at the end of the microstrip line. The net transmission coefficient without these effects proves to be expressed as follows, if the reflection coefficients Γ_1, Γ_2 looking outside from the ends of the microstrip line are small:

$$S_{21} \approx \frac{S_{21m}}{S_{21o}}(1-\Gamma_1 S_{22})(1-\Gamma_2 S_{11}) \tag{48}$$

where S_{21m} and S_{21o} are transmission coefficients measured with and without the dielectric resonator, respectively. Equation (48) means that S_{21} is approximately given by S_{21m}/S_{21o} if $\Gamma_1 S_{22}$ and $\Gamma_2 S_{11}$ are very small. In this case, precise determinations of reference planes is unnecessary if the microstrip line used is so long that $M(x)$ may decrease enough at the end of the line. In our experiments, the magnitudes of $\Gamma_1 S_{22}$ and $\Gamma_2 S_{11}$ were less than 0.04, and the above approximation yielded, at most, an error of 8 percent. Q_0' was obtained from the frequency dependence curve of $|S_{21}|$. Theoretical values of k^2 were calculated from (25) at $\omega = \omega_0$. ω_0 was determined to satisfy the boundary condition (40). When $n = 20$, ω_0 and ω_0' agreed to within 2 percent in our experiments. Fig. 6 shows the comparison between theoretical and experimental values of k^2 for three types of dielectric resonators. k^2 is given as a function of d in each figure. The theory and experiments agree well.

Fig. 7 shows the calculated values of k^2 versus d, when the upper limit of the integral in (25) is taken as a parameter. k^2 in this case is considered to indicate the coupling coefficient to the microstrip line of length $2l$. The microstrip line of a length larger than $3\lambda/2$ can be regarded to have almost the same k^2 values as that of the infinite length, as shown in Fig. 7.

V. Conclusion

The transmission characteristics of a microstrip line coupled with a cylindrical dielectric resonator has been analyzed with the assumption that the resonator couples with the microstrip line through the distributed mutual inductance. A parallel resonance equivalent circuit and a simple formula for the coupling coefficient was obtained by solving the transmission equation. The theoretical values of the coupling coefficient could be calculated by applying the method of Fourier analysis of the electromagnetic field. The calculated values exhibit good agreement with the experimental values.

Acknowledgment

The authors wish to express their thanks to T. Yamaguchi for providing dielectric resonators. They also thank Dr. Y. Makino, the Head of their laboratory, and Y. Kodera for encouragement.

References

[1] J. Cohen and M. Gilden, "Temperature stability of an MIC Gunn-effect oscillator," *IEEE Trans. Microwave Theory Tech.*, vol. MTT-21, pp. 115–116, Feb. 1973.

[2] H. Abe, Y. Takayama, A. Higashisaka, and H. Takamizawa, "A highly stabilized low-noise GaAs FET integrated oscillator with a dielectric resonator in the *C*-band," *IEEE Trans. Microwave Theory Tech.*, vol. MTT-26, pp. 156–162, Mar. 1978.

[3] T. Yamaguchi, Y. Komatsu, T. Otobe, and Y. Murakami, "Newly developed ternary (Ca, Sr, Ba) zirconate ceramic system for microwave resonators," *Ferroelectrics*, vol. 27, pp. 273–276, 1980.

[4] W. R. Day. Jr., "Dielectric resonators as microstrip-circuit elements," *IEEE Trans. Microwave Theory Tech.*, vol. MTT-18, pp. 1175–1176, Dec. 1970.

[5] T. G. Iveland, "Dielectric resonator filter for application in microwave integrated circuits," *IEEE Trans. Microwave Theory Tech.*, vol. MTT-19, pp. 643–652, July 1971.

[6] M. W. Pospieszalski, "Cylindrical dielectric resonators and their applications in TEM line microwave circuits," *IEEE Trans. Microwave Theory Tech.*, vol. MTT-27, pp. 233–238, Mar. 1979.

[7] Y. Garault and P. Guillon, "Coupling coefficient between a microstrip transmission line and a dielectric resonator disk for application to bandpass filters," in *Proc. 5th Colloquium on Microwave Communication* (vol. IV, *Microwave Circuits and Devices MT-19*), June 1974, pp. 115–164.

[8] S. B. Cohn, "Microwave bandpass filters containing high-Q dielectric resonators," *IEEE Trans. Microwave Theory Tech.*, vol. MTT-16, pp. 218–227, Apr. 1968.

[9] Korn and Korn, *Mathematical Handbook for Scientists and Engineers*. New York: McGraw-Hill, 1961.

[10] E. L. Ginston, *Microwave Measurements*. New York: McGraw-Hill, 1957.

[11] D. S. Jones, *The Theory of Electromagnetism*. New York: Pergamon, 1964, pp. 17–19.

[12] W. Schlosser and H. G. Unger, "Partially filled waveguide and surface waveguide of rectangular cross section," in *Advances in Microwave*. New York: Academic Press, 1966, vol. 1, pp. 319–387.

[13] P. Skalicky, "Coupling coefficient between dielectric resonator and microstrip line," *Electron. Lett.*, vol. 17, pp. 99–100, Jan. 1981.

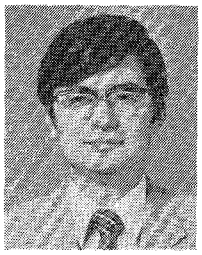

Yasutoshi Komatsu was born in Tokyo, Japan, in 1946. He received the B.S. degree in electrical engineering from University of Tokyo, Japan, in 1969.

In 1969, he joined the Sony Corporation Research Center, Yokohama, Japan. From 1969 to 1975, he worked on the development of crystal filters with high coupling resonators and on surface acoustic wave (SAW) devices. He developed a SAW filter for color TV IF circuits. He is currently engaged in the development of microwave integrated circuits, especially stabilized GaAs FET oscillators using dielectric resonators.

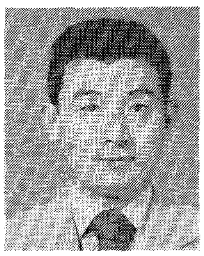

Yoshikazu Murakami was born in Aichi, Japan, in 1950. He received the B.S. degree in physics from Nagoya University, Nagoya, Japan, in 1973.

In 1974, he joined the Sony Corporation Research Center, Yokohama, Japan. From 1973 to 1980, he worked on the development of microwave integrated circuits, especially stabilized GaAs FET oscillators using dielectric resonators. He is currently engaged in the development of microwave filters using epitaxial yttrium iron garnet.

A Low-Pass Prototype Network Allowing the Placing of Integrated Poles at Real Frequencies

DAVID S. G. CHAMBERS AND JOHN DAVID RHODES, FELLOW, IEEE

***Abstract*— This paper details a procedure by which a number of attenuation poles can be placed at differing frequencies, giving an asymmetric or symmetrical response, the only restriction being that the network must be physically symmetrical. If a number of poles are placed on one side of the passband, this technique can be used to greatly increase the selectivity of a filter on this side, while maintaining an equiripple passband response.**

There are four possible arrangements for these filters. They can have even or odd degree with an even or odd number of integrated poles. Only three of these are realizable in a symmetrical network and these possibilities are dealt with individually.

An example is given in the case of an odd-degree filter with an odd number of integrated poles placed at two frequencies on opposite sides of the passband.

Manuscript received March 8, 1982; revised August 25, 1982.

The authors are with Filtronic Components Ltd., Royal London Industrial Estate, Acorn Park, Charlestown, W. Yorkshire, England.

I. Introduction

A NUMBER of microwave filter specifications call for a very low passband loss allied to extreme selectivity on one side of the band, and still requiring rejection on the

0018-9480/83/0100-0040$01.00 ©1983 IEEE